NASA TECHNICAL NOTE

NASA TN D-6555

MANNED MARS LANDER LAUNCH-TO-RENDEZVOUS ANALYSIS FOR A 1981 VENUS-SWINGBY MISSION

by Nickolas L. Faust and Thomas B. Murtagh

Manned Spacecraft Center
Houston, Texas 77058

NATIONAL AERONAUTICS AND SPACE ADMINISTRATION • WASHINGTON, D. C. • NOVEMBER 1971

1. Report No.	2. Government Accession No.	3. Recipient's Catalog No.
NASA TN D-6555		

4. Title and Subtitle	5. Report Date
MANNED MARS LANDER LAUNCH-TO-RENDEZVOUS ANALYSIS FOR A 1981 VENUS-SWINGBY MISSION	November 1971
	6. Performing Organization Code
7. Author(s)	8. Performing Organization Report No.
Nickolas L. Faust and Thomas B. Murtagh, MSC	MSC S-282
	10. Work Unit No.
9. Performing Organization Name and Address	975-11-00-00-72
Manned Spacecraft Center Houston, Texas 77058	11. Contract or Grant No.
	13. Type of Report and Period Covered
12. Sponsoring Agency Name and Address	Technical Note
National Aeronautics and Space Administration Washington, D. C. 20546	14. Sponsoring Agency Code

15. Supplementary Notes

16. Abstract

A description is given of the return of a manned Mars lander by a launch from the surface of Mars to some intermediate orbit, with subsequent maneuvers to rendezvous with a primary spacecraft (called the orbiter) in a Mars parking orbit. The type of Mars mission used to demonstrate the analytical technique includes a Venus swingby on the Mars-to-Earth portion of the trajectory in order to reduce the total mission velocity requirement. The total velocity requirement for the mission considered (if inplane launches are assumed) is approximately 5334 m/sec (17 500 ft/sec).

17. Key Words (Suggested by Author(s))	18. Distribution Statement
* Rendezvous * Rendezvous Trajectory * Optimum Trajectory * Mission Analysis * Primer Vector	

19. Security Classif. (of this report)	20. Security Classif. (of this page)	21. No. of Pages	22. Price*
None	None	23	

*For sale by the National Technical Information Service, Springfield, Virginia 22151

MANNED MARS LANDER LAUNCH-TO-RENDEZVOUS ANALYSIS FOR A 1981 VENUS-SWINGBY MISSION

By Nickolas L. Faust and Thomas B. Murtagh
Manned Spacecraft Center

SUMMARY

A manned lander vehicle may someday be used to research and explore the Mars surface. The return of this lander by way of a time-optimum launch from the Mars surface to some intermediate orbit, with subsequent maneuvers (calculated by using Lawden's primer-vector theory in an optimum multi-impulse rendezvous program) to rendezvous with the primary spacecraft in its Mars parking orbit is the subject of this report. The type of Mars mission used to demonstrate the analytical technique includes a Venus swingby on the Mars-to-Earth portion of the trajectory in order to reduce the total mission velocity requirement. The total velocity requirement, assuming inplane launches, was approximately 5334 m/sec (17 500 ft/sec) for the nominal 30-day stay on the planet surface.

INTRODUCTION

One type of Mars mission includes a Venus swingby on the Mars-to-Earth portion of the trajectory in order to reduce the total mission velocity requirement. The stay time in Mars orbit for this mission is 80 days with 30 days nominally planned for research and exploration of the Mars surface. A manned Mars lander will be used to accomplish this major scientific objective. The return of this lander to the primary spacecraft by use of a launch from the surface to some intermediate orbit, with subsequent maneuvers to rendezvous with the primary spacecraft (called the orbiter) in a Mars parking orbit, is the subject of this report.

The analysis is presented in three phases. The first phase consists of the calculation of time-optimum, constant-thrust, two-dimensional launch profiles to the intermediate orbit. Results of a parametric analysis of these launch profiles indicate the appropriate lander characteristics as well as the shape of the intermediate orbit. In the second phase, the Mars-centered inertial location of the lander in the intermediate orbit is computed, after the landing site has been specified. The mission profile provides the inertial location of the orbiter in the Mars parking orbit at the time of the lander insertion into the intermediate orbit. In the third phase, an optimum multi-impulse rendezvous program, which incorporates Lawden's primer-vector theory and a modified Davidon search routine, is used to compute the number and location of the maneuvers necessary to effect rendezvous of the lander with the orbiter. This program

optimally chooses (1) the phasing configuration for the two spacecraft before the first impulse, (2) the position and times for all intermediate impulses, and (3) the transfer time for the rendezvous. The velocity requirement for ascent (assuming inplane launches) is computed, and the rendezvous requirement then is plotted as a function of stay time on the Mars surface to produce the overall launch-window profile for the lander. A detailed description of the sequence of events from launch to rendezvous on the nominal launch day also is presented.

As an aid to the reader, where necessary the original units of measure have been converted to the equivalent value in the Système International d' Unités (SI). The SI units are written first, and the original units are written parenthetically thereafter.

SYMBOLS

A	lander cross-sectional area
C	magnitude of the intermediate impulse during lander ascent
C_D	lander drag coefficient
G	gravitational field $f(x)$, a function of position only
$g(Z_o, t_o)$	initial boundary function
H	Hamiltonian on a coasting arc
$h(Z_f, t_f)$	terminal boundary function
h	spacecraft altitude
h_a	apoapsis altitude
h_p	periapsis altitude
I_{sp}	lander ascent-engine specific impulse
J	impulsive cost, sum of the magnitudes of the applied impulse velocities for the N impulses
N	number of impulses
q	dynamic pressure
r_a	apoapsis radius of an orbital ellipse

r_p	periapsis radius of an orbital ellipse
T	lander thrust
$\boldsymbol{T}$	two-impulse Lambert reference trajectory
t	time
V	velocity
V_c	characteristic velocity
V_R	radial velocity
V_T	tangential velocity
W	lander weight
X	displacement
Z	augmented state vector (composed of the radial and tangential velocities, the radial and angular position, and the corresponding Lagrange multipliers) of the lander
z	vector composed of the components of the intermediate position vector, the time of intermediate impulse, the initial time, and the final time
β	pitch angle
γ	vernal equinox
Δt	change in time
ΔV	change in velocity
$\delta( )$	small deviation or perturbation of parameter ( )
η	true anomaly
θ	misalinement in line of apsides
λ	primer vector given by Lawden's optimality condition
ν	unit vector in the direction of the intermediate impulse during lander ascent
τ	orbital period
ϕ	phase angle

Subscripts:

A	refers to spacecraft A
B	refers to spacecraft B
f	refers to the final condition or state of the parameter
m	refers to the condition or state at some point between the initial and final condition or state of the parameter
o	refers to the initial condition or state of the parameter

Superscripts:

'	refers to a parameter on the perturbed trajectory
+	indicates a parameter value immediately after time t
-	indicates a parameter value immediately before time t

Operators:

$(\dot{})$	derivative of the parameter with respect to time, d/dt
∇	gradient

REFERENCE MISSION

A heliocentric plot of the 1981 Mars-stopover/Venus-swingby mission used for the analysis presented in this report is shown in figure 1. The Earth-departure sequence (computed by using the multi-orbit injection technique discussed in ref. 1) begins with lift-off on November 7, 1981, with the trans-Mars injection maneuver occurring 67 hours later. The Earth-to-Mars flight time is 266 days. The Mars orbit insertion (MOI) maneuver places the spacecraft in a 370- by 11 708-kilometer (200 by 6322 nautical miles) orbit inclined 75° with respect to the Mars equator. The landing operations begin 20 days after MOI and result in a landing at 69° N 130° E. The nominal surface stay time is 30 days, and the total orbital stay time is 80 days. The parking orbit is designed to provide proper alinement for Mars departure (ref. 2). The Mars-to-Venus flight time is 127 days, with the point of closest approach to Venus being 4722 kilometers (2550 nautical miles). The Venus-to-Earth flight time is 169 days, and the Earth-entry velocity at an altitude of 121 920 meters (400 000 feet) is 12 048 m/sec (39 530 ft/sec).

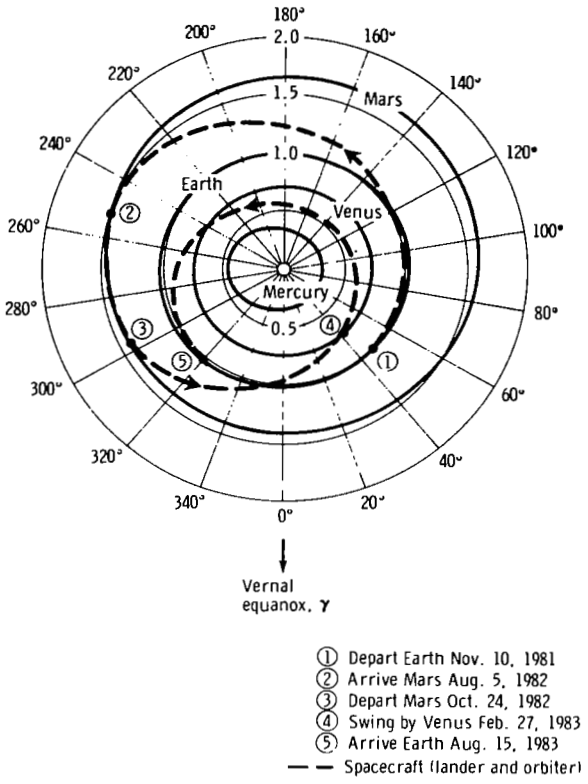

Figure 1. - Heliocentric view of a 1981 80-day Mars-stopover/Venus-swingby mission.

DISCUSSION OF NUMERICAL RESULTS

Launch to Intermediate Orbit

The nonlinear ordinary differential equations of motion for the time-optimum, constant-thrust, two-dimensional lander launch-trajectory computation is contained in reference 3. The control variable is the thrust orientation with respect to the local horizontal. The Mars-atmosphere model used for the analysis is the mean density profile presented in reference 4. The lander drag coefficient C_D and cross-sectional area A were assumed to be constant. The Euler-Lagrange (costate) differential equations can be derived from equations presented in reference 3. The method of perturbation functions (ref. 3) was used to generate the numerically converged solutions. This technique, which is an indirect method based on the conditions required for mathematical optimality, is designed to satisfy these conditions by various iterative procedures. The boundary conditions for the state and costate differential equations can be expressed as $g(Z_o, t_o) = 0$ and $h(Z_f, t_f) = 0$, where t_o and t_f represent the initial and final times, respectively, and Z is an augmented state vector composed of the radial and tangential velocities, the radial and angular position, and the corresponding Lagrange multipliers. The numerical integration of the state and costate equations with some Z_o generally will produce an $h(Z_f, t_f)$ that is nonzero. The error in the terminal constraint vector must be related mathematically to the initial conditions to begin the iteration procedure that will converge on the desired solution. The minimum-norm correction procedure derived and discussed in reference 5 was used to produce the converged solutions presented in this report.

For the data presented, the lander ascent-engine specific impulse I_{sp} was fixed at 380 seconds, and the initial lander ballistic parameter $W_o/(C_D A)$ was chosen to be 19.15×10^3 N/m^2 (400 lb/ft^2). The apoapsis altitude h_a of the intermediate ellipse was always 185.2 kilometers (100 nautical miles).

The characteristic velocity V_c for the time-optimum (free argument of periapsis) transfer from the termination of a vertical rise to a 91-meter (300 feet) altitude to the specified intermediate orbit is presented in figure 2 as a function of the true

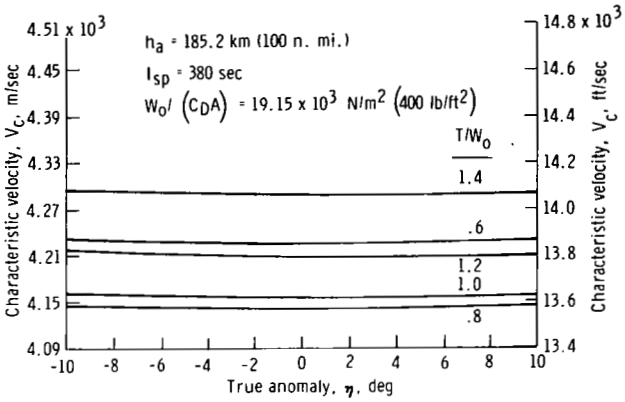

(a) h_p = 91 440 meters (300 000 feet).

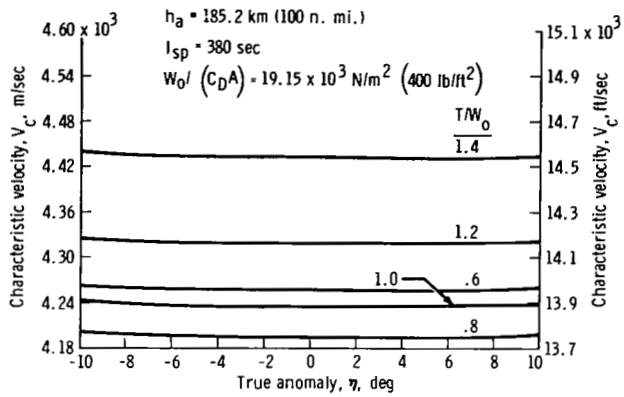

(b) h_p = 106 680 meters (350 000 feet).

Figure 2. - Lander characteristic velocity as a function of true anomaly.

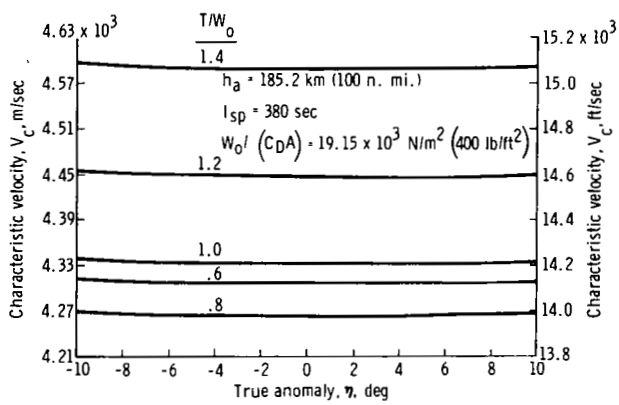

(c) h_p = 121 920 meters (400 000 feet).

Figure 2. - Concluded.

anomaly η at intermediate-orbit insertion. The curves were generated for initial thrust-to-weight ratios T/W_o between 0.6 and 1.4. Periapsis altitudes h_p of 91 440, 106 680, and 121 920 meters (300 000, 350 000, and 400 000 feet) were considered. Lower periapsis altitudes would have produced undesirable orbit-decay times for the lander intermediate orbit. It should be noted from these curves that the performance (measured by V_c) is insensitive to variations in true anomaly between $\pm 10°$. Consequently, the choice of the true-anomaly angle at the intermediate-orbit-insertion point can be arbitrary within $\pm 10°$. With $\eta = 5°$, the characteristic velocity was plotted against T/W_o in figure 3. The minimum V_c occurs for the lowest periapsis altitude because the apoapsis altitude is fixed at 185.2 kilometers (100 nautical miles), and the minimum of that curve occurs for $0.8 \leq T/W_o \leq 1.0$. Based on these data, the periapsis altitude of the intermediate ellipse was chosen to be 91 440 meters (300 000 feet) (for $\eta = 5°$), and the initial T/W_o was 1. The ascent-parameter profiles and dynamic-pressure profile for this case are illustrated in figure 4.

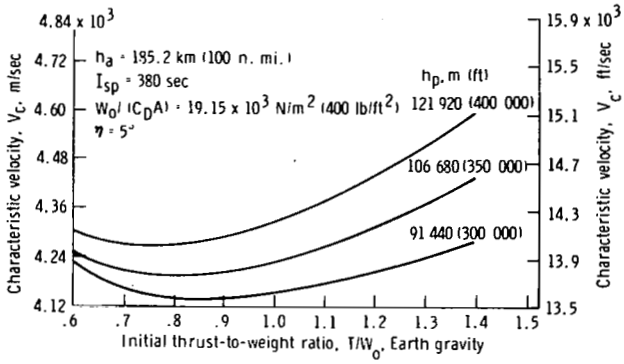

Figure 3.- Lander ascent performance as shown by the characteristic velocity as a function of the initial thrust-to-weight ratio.

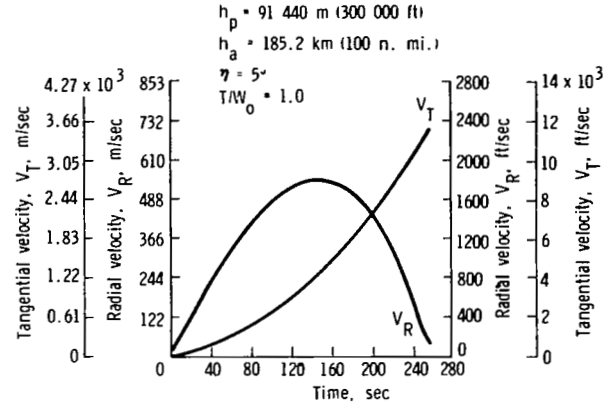

(a) Radial and tangential velocity as a function of time.

Figure 4.- Typical ascent profile.

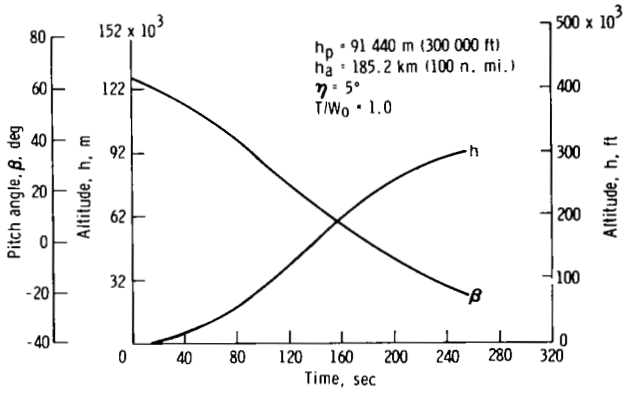

(b) Altitude and pitch angle as a function of time.

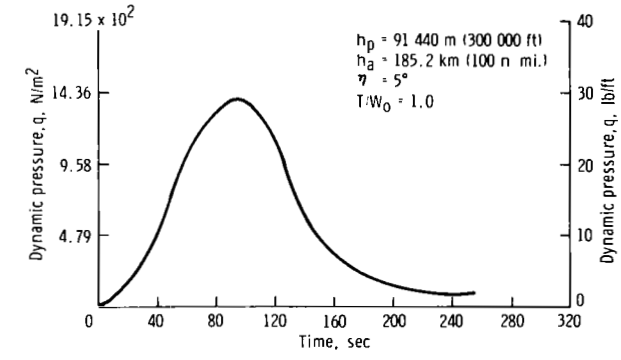

(c) Dynamic pressure as a function of time.

Figure 4.- Concluded.

Geometry of an Inplane Launch

The assumption of an inplane launch simplifies the algebra required for the analysis and, in most cases, produces a lower velocity requirement for the lander to rendezvous with the orbiter. The inplane-launch assumption provides two launch opportunities per day, one toward the north and one toward the south. Spherical trigonometry may be used to compute the Mars-centered inertial location of the lander at intermediate-orbit insertion once the landing site has been specified. The mission profile provides the inertial location of the orbiter in the Mars parking orbit at the time of the lander insertion into the intermediate orbit.

Initialization of the Rendezvous Phase

After the lander has inserted into an intermediate orbit, the rendezvous phase begins. The orbital orientations for the northerly and southerly launches differ, and the initial phase angle (central angle between the lander and the orbiter) at lander insertion depends on the day and time of launch. The nodal and apsidal rates are incorporated in the orbiter equations of motion until the launch day. For a specific launch day, the nodal and apsidal locations of the orbiter are fixed for both daily launches (two-body motion); these perturbation effects are assumed to be negligible for the rendezvous analysis.

Method of Solution

The basis for the N-impulse open-time rendezvous problem originated when the necessary conditions for an optimum trajectory were derived by Lawden (ref. 6). This work was extended by Lion and Handelsman (ref. 7) to nonoptimum trajectories with the development of a method to determine when a reference N-impulse trajectory could be improved in cost by an (N + 1) impulse trajectory. Cost is defined as the sum of the magnitudes of the applied impulses and is discussed in the appendix.

A gradient-type differential cost function that indicates the way to improve the reference solution for a fixed-time, fixed-state problem is presented in reference 7. These results were combined by Jezewski and Rozendaal (ref. 8) with a modified Davidon multivariable search routine (refs. 9 and 10). This multivariable search routine uses a one-dimensional search (ref. 11) as well as an accelerated gradient method to find a local extremal. An extension of the theory to an N-impulse, fixed-time problem that allows the optimization method to choose the true anomaly for leaving the initial orbit and for arriving on the final orbit is presented in reference 12. For this report, a further extension to the theory has been made (discussed in the appendix) that results in an open-time rendezvous-type solution. With a specified reference trajectory between an active spacecraft A and a passive spacecraft B, this method optimally chooses the phasing configuration of the two spacecraft, the positions and times of all intermediate impulses, and the transfer time needed for the rendezvous. A local minimum is ensured by this procedure. To guarantee that no solutions with extremely long transfer times would be chosen, a maximum total time boundary ($t_{\text{coast in initial orbit}} + t_{\text{transfer}}$) of 24 hours was imposed on the solutions.

It should be noted that this procedure yields only local minimums and not global minimums. This characteristic is inherent in the search procedure that is used, which assumes a unimodal function. (Unimodality is defined in ref. 13 as "in precise mathematical terms, functions y of a single variable x which, roughly speaking, have only one hump in the interval to be explored.") To overcome this difficulty, a series of solutions had to be obtained — each one a local minimum in a different area of the N-impulse solution space.

Application of the Method

To explain this concept further, spacecraft A and B must be considered in the respective coplanar ellipses with coinciding lines of apsides. If the spacecraft were

allowed to move in orbit to the optimum point or points for arrival and departure (optimal fixed-time trajectories with free true anomalies), the search procedure would arrive at four types of extremals — periapsis-to-periapsis transfer, periapsis-to-apoapsis transfer, apoapsis-to-periapsis transfer, and apoapsis-to-apoapsis transfer.

With the same problem treated as a rendezvous problem (positions on initial and final orbits are linked by time) with a fixed transfer time, the cost of the solutions would depend on the phasing of spacecraft A and B at the beginning of the problem. If spacecraft A were allowed to coast Δt_A hours in orbit to periapsis, spacecraft B would have to move Δt_A hours plus the fixed transfer time in its orbit. The position of spacecraft B in orbit is not likely to be near one of the optimum places for rendezvous.

Addition of the open-time capability (discussed in the appendix) to the rendezvous technique represents another problem. The open-time problem with an upper bound on total time may permit spacecraft A to coast to an orbital apsidal point at Δt_A hours and to vary the transfer time so that spacecraft B may seek an apsidal point on its orbit at time Δt_B. Thus, the transfer time for the maneuver will be $\Delta t_B - \Delta t_A$ for $\Delta t_B > \Delta t_A$. If the period τ_B of the spacecraft B orbit is much longer than the period τ_A of the spacecraft A orbit, multiple extremals may be found. For example, if $\Delta t_A + \tau_A < \Delta t_B$, then another solution will be found with transfer times of $\Delta t_B - (\Delta t_A + \tau_A)$. These solutions form an envelope from which the minimum-cost trajectory between the two extremal points may be selected. The time increments Δt_A and Δt_B are measured from the reference time.

Nominal Results

The nominal day of launch for the selected reference mission will now be considered. The northerly launch will be examined first. The respective orbital orientations of the lander and orbiter at the time of the lander orbit insertion are shown in figure 5. It should be noted that the lander orbit is nearly circular while the orbiter orbit has a 0.5996 eccentricity. The misalinement of the line of apsides is 43.5°. The near-circular lander orbit does not have well-defined periapsis and apoapsis extremals. This observation is supported by the results of this study, which indicate that, by using this method, the lander should leave at a point on its ellipse so that the total transfer angle between the lander (at the firing of the first impulse) and the orbiter (at rendezvous) is approximately 360°. Some solutions to periapsis and apoapsis of the orbiter orbit were found with 180° transfers, but these solutions were similar in cost to data already presented and sometimes degenerated into solutions already found. In most cases, the generated solutions were three-impulse solutions, but some two-impulse solutions were found. In figure 6, the impulsive ΔV required for the northerly launch is shown as a function of the amount of time Δt_A the lander would remain in orbit before firing the first impulse for rendezvous. The curves are numbered to differentiate types of solutions. Curve 1 represents the envelope of open-time rendezvous solutions in which the lander leaves its orbit at approximately 43° and rendezvouses with the

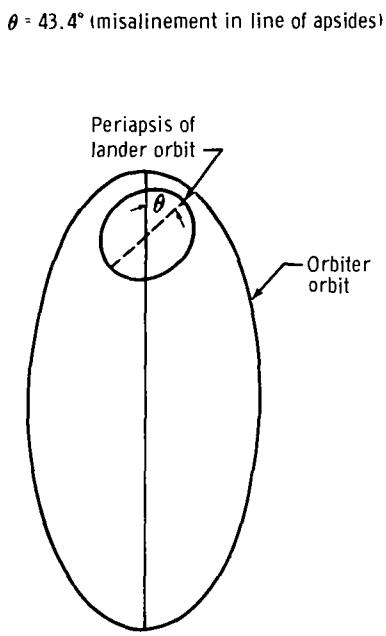

Figure 5. - Initial orbital orientation for a northerly nominal launch.

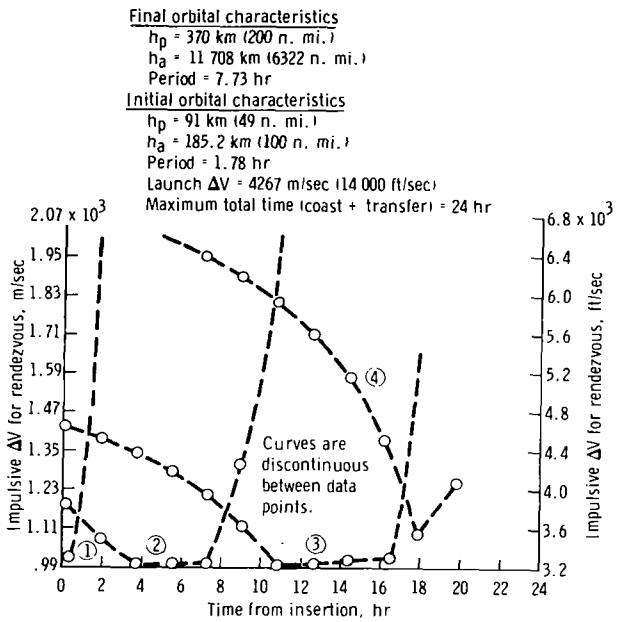

Figure 6. - Lander coast time in initial orbit before the first impulse for a northerly launch.

orbiter when the orbiter first reaches periapsis 3.04 hours after lander insertion. The individual points on this curve are ΔV minimums for the lander leaving its orbit the first time of arrival at the departure point, the second time, and so on. The other curves also are envelopes of this type. Curve 2 is the envelope of solutions in which the lander leaves its orbit at approximately the same point as before but does not rendezvous until the orbiter has reached periapsis the second time at 10.77 hours. Curve 3 is the same type of envelope, except that the rendezvous occurs after the orbiter has reached periapsis a third time (18.50 hours). The maximum time boundary of 24 hours will not permit enough time for the orbiter to reach its extremal point again. Curve 4 is the envelope of open-time rendezvous solutions from the lander orbit to the third time the orbiter reaches its extremal at apoapsis. It should be noted from the transfer-to-periapsis envelopes that the minimums of all three curves have approximately the same ΔV. The difference exists only in the phasing, but, because the lander orbit is nearly circular, the ΔV penalty for phasing differences is small. The same effect is observed for the apoapsis curves. Thus, only one curve is presented.

The initial orientation of the lander and orbiter orbits is shown in figure 7. Data similar to those in figure 6 are presented in figure 8 for the southerly launch on the nominal launch day. The identification of the envelopes is the same as before, but the lowest ΔV for the southerly launch is somewhat higher than the northerly launch minimum.

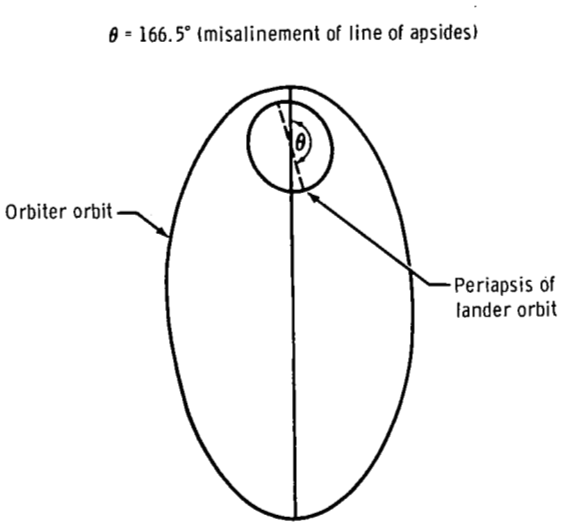

Figure 7. - Initial orbital orientation for a southerly nominal launch.

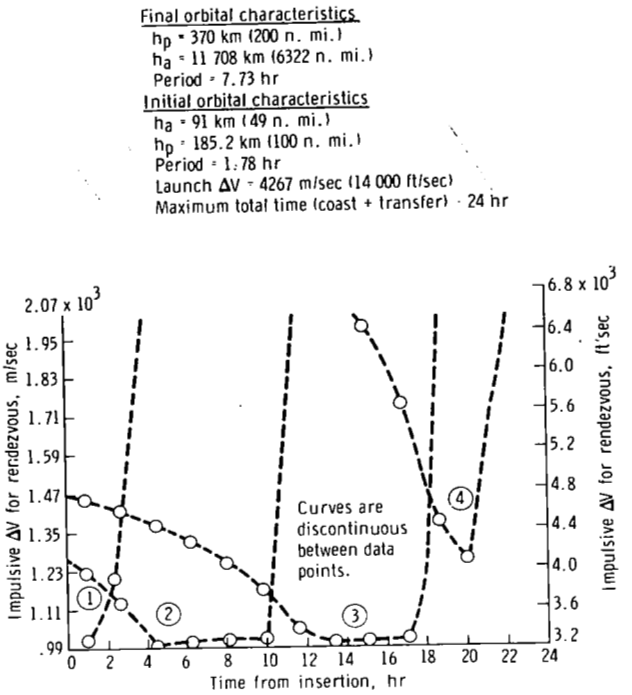

Figure 8. - Lander coast time in initial orbit before the first impulse for a southerly launch.

The lower of the two minimums for the nominal launch is chosen, and that solution is used for the nominal launch profile. This profile is presented in some detail. The impulsive ΔV needed for the rendezvous phase is 980 m/sec (3214 ft/sec). The time from insertion to rendezvous is 18.5 hours. In figure 9, the altitudes of the lander and the orbiter are plotted from after the first impulse to rendezvous. The rendezvous-range time history from lander insertion to rendezvous is shown in figure 10; a time history of the phasing from lander insertion to rendezvous, in figure 11; and the effect of each impulse on the lander orbit until rendezvous, in figure 12. In figure 12, the first impulse is shown to alter the line of apsides of the lander orbit to within 2.6° of the orbiter orbit and to raise the apoapsis altitude by 11 088 kilometers (5987 nautical miles). The second impulse further alines the lines of apsides and raises the periapsis of the lander orbit to 370 kilometers (200 nautical miles). The third impulse completes the rendezvous.

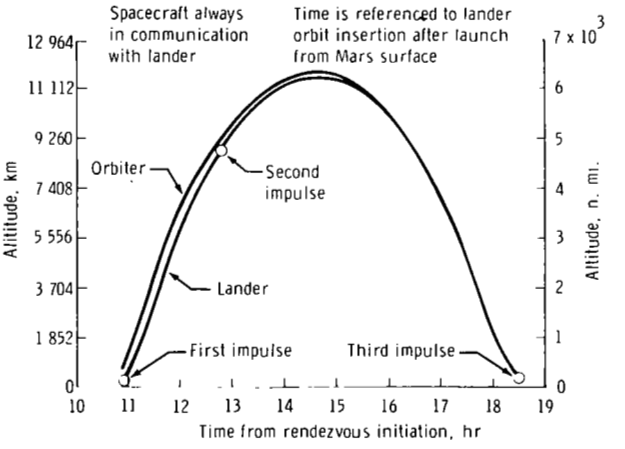

Figure 9. - Altitude time history for the terminal phase of the rendezvous.

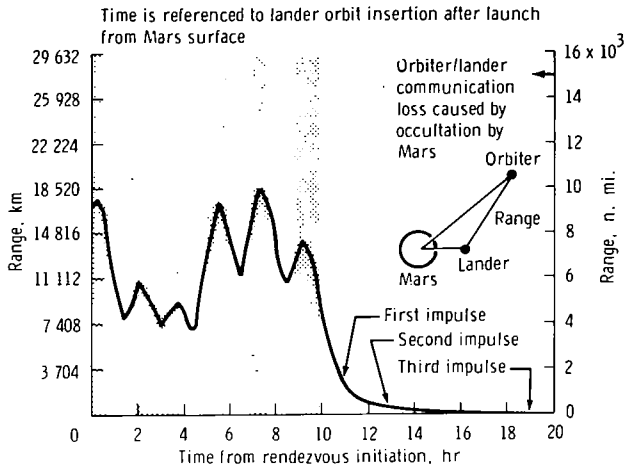

Figure 10. - Rendezvous-range time history.

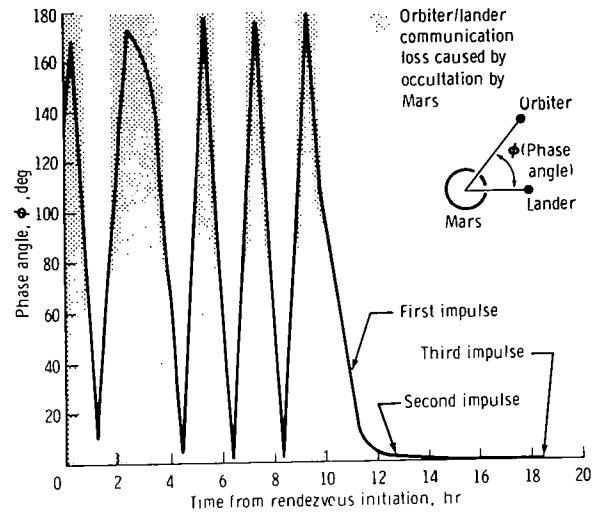

Figure 11. - Rendezvous-phasing time history.

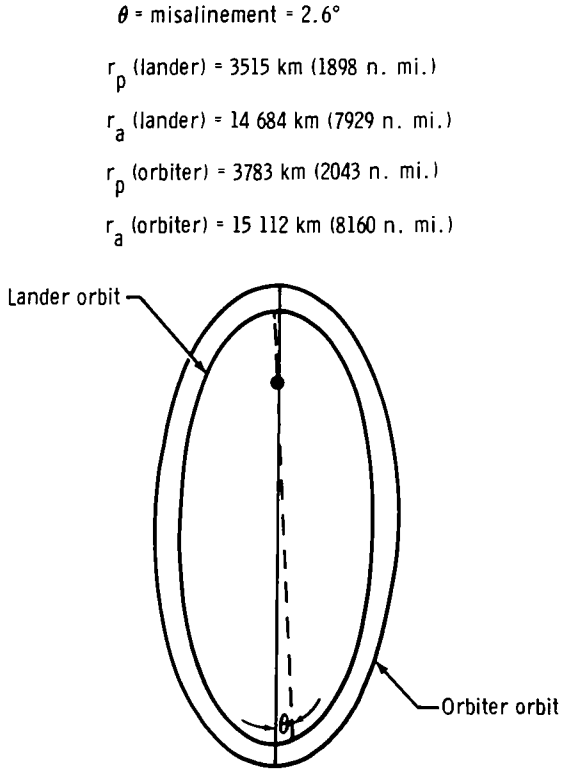

(a) Orbital configuration after the first impulse.

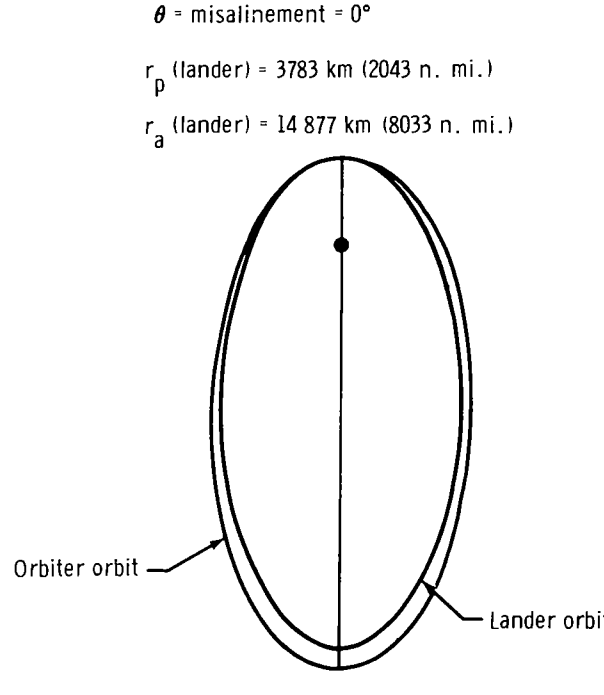

(b) Orbital configuration after the second impulse.

Figure 12. - Orbital-transfer geometry.

r_p (lander) = r_p(orbiter) = 3783 km (2043 n. mi.)

r_a(lander) = r_a (orbiter) = 15 112 km (8160 n. mi.)

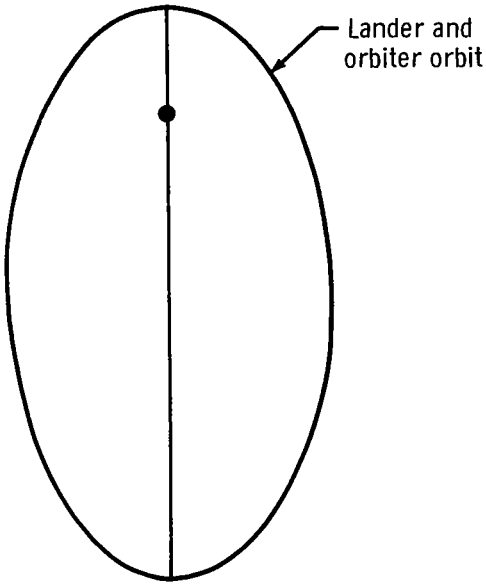

(c) Orbital configuration after the third impulse.

Figure 12. - Concluded.

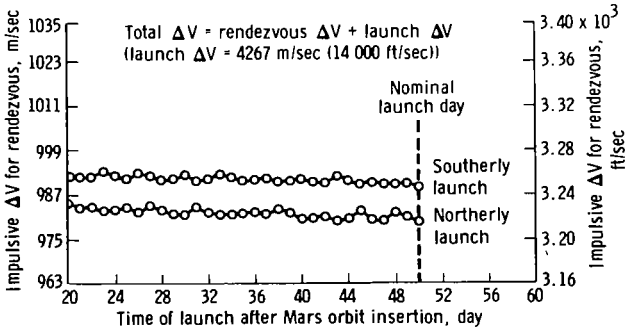

Figure 13. - Rendezvous ΔV as a function of launch day.

Data for Total Launch to Rendezvous

The daily minimum ΔV for launch from the Mars surface to rendezvous during the nominal launch day has been found, and launches for other days of the launch window now will be investigated. Because each northerly launch has the same line of apsides for the lander orbit, the only change in the alinement for northerly launches for all days of the launch window is caused by the regression of the nodes and by the apsidal rate of the orbiter orbit. The daily alinement change for the southerly launches is caused by the same effect. Also, each launch day (northerly and southerly launches) has a different initial-phasing configuration than any other day. Thus, because the launches are inplane and because the lander orbit is the same for each day, it should not be assumed that one launch-window ΔV will be constant for all northerly launches and another ΔV will be constant for all southerly launches. Discussion of the phasing for the nominal launch day indicates that there should be variation in cost based on the initial changes in phasing and some based on the apsidal change from day to day. The cost (excluding launch ΔV) for northerly and southerly launches for the total Mars lander launch window is presented in figure 13, which represents the results of this analysis. For comparison, the ΔV for the coplanar, alined line-of-apsides case was calculated to be 970 m/sec (3181 ft/sec). The southerly launch ΔV is greater than that for the northerly launch because of the greater misalinement of the line of apsides.

CONCLUSION

Use of an optimum finite-thrust launch program and an optimum multi-impulse rendezvous program has made it possible to determine a quasi-optimum lander ΔV profile for the launch window of the 1981 Venus-swingby Mars mission. Inplane launches were assumed to facilitate computation, but phasing considerations and orbital apsidal misalinements were incorporated in the study. Results were presented in detail for the nominal launch day, and the optimum rendezvous for that day was discussed. The total launch-to-rendezvous ΔV data indicate a fairly constant rendezvous ΔV of approximately 5334 m/sec (17 500 ft/sec) with small variations caused by phasing and apsidal misalinement.

Manned Spacecraft Center
National Aeronautics and Space Administration
Houston, Texas, June 1, 1971
975-11-00-00-72

REFERENCES

1. McAdoo, Stewart F., Jr.; and Funk, Jack: An Earth Departure Technique for Use in Manned Interplanetary Missions Using the NERVA Engine. AAS preprint 70-039, presented at the 16th Annual Meeting of the Am. Astronaut. Soc. (Anaheim, Calif.), June 8-10, 1970.

2. Thibodeau, Joseph R., III: Use of Planetary Oblateness for Parking Orbit Alinement. NASA TN D-4657, 1968.

3. Lewallen, Jay M.: An Analysis and Comparison of Several Trajectory Optimization Methods. Ph. D. Dissertation, The Univ. of Texas at Austin, 1966.

4. Anon.: Models of Mars Atmosphere (1967). NASA SP-8010, 1968.

5. Lewallen, J. M.; Tapley, B. D.; and Williams, S. D.: Iteration Procedures for Indirect Trajectory Optimization Methods. J. Spacecraft Rockets, vol. 5, no. 3, Mar. 1968, pp. 321-327.

6. Lawden, D. F.: Optimal Trajectories for Space Navigation. Butterworth & Co. (Publishers) Ltd. (London), 1963.

7. Lion, P. M.; and Handelsman, M.: Primer Vector on Fixed-Time Impulsive Trajectories. AIAA, vol. 6, no. 1, Jan. 1968, pp. 127-132.

8. Jezewski, D. J.; and Rozendaal, H. L.: An Efficient Method for Calculating Optimal Free-Space N-Impulse Trajectories. AIAA, vol. 6, no. 11, Nov. 1968, pp. 2160-2165.

9. Davidon, William C.: Variable Metric Method for Minimization. Rept. ANL-5990 (Rev.), Argonne Natl. Lab., Nov. 1959.

10. Fletcher, R.; and Powell, M. J. D.: A Rapidly Convergent Descent Method for Minimization. Computer J., vol. 6, no. 2, July 1963, pp. 163-168.

11. Johnson, Ivan L., Jr.: Impulsive Orbit Transfer Optimization by an Accelerated Gradient Method. J. Spacecraft Rockets, vol. 6, no. 5, May 1969, pp. 630-632.

12. Jezewski, Donald J.: A Method for Determining Optimal Fixed-Time N-Impulse Trajectories Between Arbitrarily Inclined Orbits. No. AD 30, proceedings of the 19th Congress of the Int. Astronaut. Fed. (New York, N. Y.), Oct. 13-19, 1968.

13. Wilde, Douglass J.: Optimum-Seeking Methods, Prentice-Hall, Inc., Englewood Cliffs, N.J., 1964, p. 10.

APPENDIX

DEVELOPMENT OF OPEN-TIME RENDEZVOUS CAPABILITY

In the calculation of optimum N-impulse trajectories for open-time rendezvous, a reference solution must first be established, the cost of which may be improved by perturbations. The impulsive cost J is defined as the sum of the magnitudes of the applied impulse velocities for the N impulses.

$$J = \sum_{i=1}^{N} |\Delta V_i| \tag{A1}$$

The reference solution T is assumed to be the two-impulse Lambert reference trajectory between orbits A and B that is formed by applying impulses ΔV_o and ΔV_f at the times t_o and t_f, respectively. A perturbation in position δX_m is applied at time t_m ($t_o < t_m < t_f$) to the reference trajectory, which results in the perturbed trajectory T' with velocity perturbations δV_o^- and δV_f^+, where the minus indicates an event immediately before time t and the plus indicates an event immediately after time t. The δV_o^- and δV_f^+ are needed to consider the variations in the initial and final orbits, respectively, caused by the perturbation.

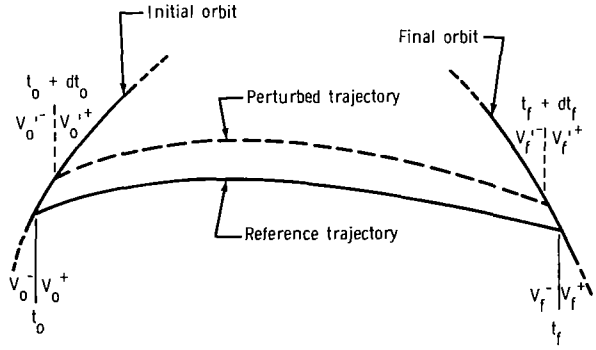

Figure A-1. - Generalized rendezvous-problem geometry.

For the rendezvous open-time problem, the velocities on the ends of the perturbed orbit are as follows (fig. A-1).

$$V_o'^- = V_o^- + \dot{V}_o^- dt_o \tag{A2a}$$

$$V_o'^+ = V_o^+ + \delta V_o + \dot{V}_o'^+ dt_o \tag{A2b}$$

$$V_f'^- = V_f^- + \delta V_f^- + \dot{V}_f'^- dt_f \tag{A2c}$$

$$V_f'^{+} = V_f^{+} + \dot{V}_f^{+} dt_f \tag{A2d}$$

The $\dot{V}\,dt$ terms account for the movement in the orbits and for the change in the arrival and departure times related to this movement.

Thus, the differential cost between the reference and perturbed trajectories is

$$dJ = J' - J \tag{A3}$$

where

$$J = \left|V_o^{+} - V_o^{-}\right| + \left|V_f^{+} - V_f^{-}\right| \tag{A4a}$$

$$J' = \left|V_o'^{+} - V_o'^{-}\right| + \left|\delta V_m^{+} - \delta V_m^{-}\right| + \left|V_f'^{+} - V_f'^{-}\right| \tag{A4b}$$

where $\left|\delta V_m^{+} - \delta V_m^{-}\right|$ is the absolute value of the difference in velocity on the two conics of the perturbed solution at time t_m. By assuming small perturbations in a gravitational field of the form $G = f(x)$, where x is a position, and by retaining first-order terms, equation (A3) becomes

$$dJ = \lambda_o \cdot \delta V_o^{+} - \lambda_f \cdot \delta V_f^{-} + \left|\delta V_m^{+} - \delta V_m^{-}\right| \tag{A5}$$

where λ_o and λ_f are the values of the primer vector λ given by Lawden's optimality condition. Lawden's optimality condition states that at the time of an impulse, the primer vector is alined with the impulse and has a constant magnitude. This constant magnitude is defined arbitrarily as unity by making the boundary conditions

$$\lambda(t_o) = \lambda_o = \Delta V_o / \left|\Delta V_o\right| \tag{A6a}$$

$$\lambda(t_f) = \lambda_f = \Delta V_f / \left|\Delta V_f\right| \tag{A6b}$$

The adjoint equation (a relationship linking the perturbations to the adjoint variables $(\lambda, -\dot{\lambda})$) is

$$(\lambda \cdot \delta V) - (\dot{\lambda} \cdot \delta X) = \text{constant} \tag{A7}$$

A method for computing $\dot{\lambda}$, the primer-vector derivative, is contained in reference 7.

By use of equation (A7), evaluated at the boundaries of the two conics of T', equation (A5) may be transformed into

$$dJ = \dot{\lambda}_o^+ \cdot \delta X_o^+ - \dot{\lambda}_f^- \cdot \delta X_f^- + \lambda_m^- \cdot \delta V_m^- - \dot{\lambda}_m^- \cdot \delta X_m^-$$

$$- \lambda_m^+ \cdot \delta V_m^+ + \dot{\lambda}_m^+ \cdot \delta X_m^+ + \left| \delta V_m^+ - \delta V_m^- \right| \tag{A8}$$

Because λ and $\dot{\lambda}$ are computed on the reference and, therefore, are continuous, $\lambda_m^+ = \lambda_m^- = \lambda_m$ and $\dot{\lambda}_m^+ = \dot{\lambda}_m^- = \dot{\lambda}_m$. Also, $\delta X_m^+ = \delta X_m^-$ for continuity of the position vector at t_m. Therefore, equation (A8) becomes

$$dJ = \lambda_o \cdot \delta X_o^+ - \lambda_f \cdot \delta X_f^- + C(1 - \lambda_m \cdot \nu) \tag{A9}$$

where C is the magnitude of the intermediate impulse and ν is a unit vector in its direction. The arrival and departure times of the original orbits control the end-point motion through the equations

$$dX = \delta X + V\, dt \tag{A10a}$$

or, for this discussion

$$\delta X_o^+ = dX_o - V_o^+ dt_o \tag{A10b}$$

and

$$\delta X_f^- = dX_f - V_f^- dt_f \tag{A10c}$$

because

$$dX_o = V_o^- dt_o \tag{A11a}$$

$$dX_f = V_f^+ dt_f \tag{A11b}$$

$$\delta X_o^+ = -\left(V_o^+ - V_o^-\right) dt_o \tag{A11c}$$

$$\delta X_f^- = \left(V_f^+ - V_f^-\right) dt_f \tag{A11d}$$

When this equation is substituted into equation (A9), the cost differential becomes

$$dJ = C\left(1 - \lambda_m \cdot \nu\right) - \dot{\lambda}_o^+ \cdot \left(V_o^+ - V_o^-\right) dt_o - \dot{\lambda}_f^- \cdot \left(V_f^+ - V_f^-\right) dt_f \tag{A12}$$

or

$$dJ = C\left(1 - \lambda_m \cdot \nu\right) - \left|\Delta V_o\right|\left(\dot{\lambda}_o^+ \cdot \lambda_o\right) dt_o - \left|\Delta V_f\right|\left(\dot{\lambda}_f^- \cdot \lambda_f\right) dt_f \tag{A13}$$

The conditions for improvement of the reference solution are obtained by inspection of equation (A13).

1. If $\dot{\lambda}$ at t_o and t_f is zero or orthogonal to λ_o and λ_f and if $|\lambda_m| > 1$, the solution will be improved by adding an impulse in the direction of λ_m at t_m.

2. If $\dot{\lambda}$ at t_o and t_f is not orthogonal to λ_o and λ_f and is nonzero and if $|\lambda_m| > 1$, the solution can be improved by perturbing the initial and final conditions and by adding an impulse in the direction of λ_m at t_m.

3. If $\dot{\lambda}$ at t_o and t_f is not orthogonal to λ_o and λ_f and is nonzero and if $|\lambda_m| < 1$, the solution can be improved by perturbing the initial and final conditions.

Condition 2 is the most general of the conditions; conditions 1 and 3 are subclasses of condition 2.

The reference trajectory now is assumed to be a three-impulse trajectory T that is perturbed to obtain a T'. The differential cost (developed similarly to eq. (A9)) is

$$dJ = \dot{\lambda}_o^+ \cdot \delta X_o^+ - \dot{\lambda}_f^- \cdot \delta X_f^- - \dot{\lambda}_m^- \cdot \delta X_m^- - \lambda_m \cdot \left(\delta V_m^+ - \delta V_m^-\right)$$

$$+ \dot{\lambda}_m^+ \cdot \delta X_m^+ + \left|\delta V_m^+ - \delta V_m^-\right| \tag{A14}$$

For the three-impulse reference, the primer vector λ_m is chosen to be a unit vector in the direction of the intermediate impulse $(\delta V_m^+ - \delta V_m^-)$ so that the fourth and sixth terms of equation (A14) vanish. The position vector X_m must be continuous, and, because the time at which the intermediate impulse is applied varies between the perturbed and reference trajectories, the total change in X_m is

$$dX_m = \delta X_m^- + \dot{X}_m^- dt_m \tag{A15a}$$

$$dX_m = \delta X_m^+ + \dot{X}_m^+ dt_m \tag{A15b}$$

When equation (A15) is substituted into equation (A14), the cost function becomes

$$dJ = \dot{\lambda}_o^+ \cdot \delta X_o^+ - \dot{\lambda}_f^- \cdot \delta X_f^- + \left(\dot{\lambda}_m^+ - \dot{\lambda}_m^-\right) \cdot dX_m$$

$$- \left(\dot{\lambda}_m^+ \cdot \dot{X}_m^+ - \dot{\lambda}_m^- \cdot \dot{X}_m^-\right) dt_m \tag{A16}$$

By use of equation (A11), equation (A16) becomes

$$dJ = -\dot{\lambda}_o^+ \cdot \left(V_o^+ - V_o^-\right) dt_o - \dot{\lambda}_f^- \cdot \left(V_f^+ - V_f^-\right) dt_f$$

$$+ \left(\dot{\lambda}_m^+ - \dot{\lambda}_m^-\right) \cdot dX_m - \left(\dot{\lambda}_m^+ \cdot \dot{X}_m^+ - \dot{\lambda}_m^- \cdot \dot{X}_m^-\right) dt_m \tag{A17}$$

By use of equation (A6), equation (A17) becomes

$$dJ = -\dot{\lambda}_o^{+} \cdot \lambda_o |\Delta V_o| dt_o - \dot{\lambda}_f^{-} \cdot \lambda_f |\Delta V_f| dt_f + \left(\dot{\lambda}_m^{+} - \dot{\lambda}_m^{-}\right) \cdot dX_m$$

$$- \left(\dot{\lambda}_m^{+} \cdot \dot{X}_m^{+} - \dot{\lambda}_m^{-} \cdot \dot{X}_m^{-}\right) dt_m \tag{A18}$$

The Hamiltonian on a coasting arc is

$$H = \lambda \cdot \dot{V} - \dot{\lambda} \cdot V \tag{A19}$$

equation (A19) now becomes

$$dJ = -\dot{\lambda}_o^{+} \cdot \lambda_o |\Delta V_o| dt_o - \dot{\lambda}_f^{-} \cdot \lambda_f |\Delta V_f| dt_f + \left(\dot{\lambda}_m^{+} - \dot{\lambda}_m^{-}\right) \cdot dX_m + \left(H_m^{+} - H_m^{-}\right) dt_m \tag{A20}$$

equation (A20) then can be written in the form

$$dJ = \nabla J \cdot dz \tag{A21}$$

where ∇ is the gradient operator and the vector z for three impulses is composed of the components of the intermediate position vector, the time of intermediate impulse, the initial time, and the final time. Further discussion on the method of minimization is found in reference 10.